Effect of Water on the Oxygen Barrier Properties of Polyethylene Terephthalate and Poly(lactide) Films

Rafael Auras, Bruce Harte, Susan Selke*

School of Packaging, MSU, East Lansing, MI. 48824-1223, USA
*Correspondence to: Phone: 517-3533367; Fax: 517-3538999; E-mail: aurasraf@msu.edu

Summary. Modern technologies of producing poly(lactide), PLA, are lowering production costs, so PLA is now potentially available for use as a food packaging material. PLA has been used in containers for fresh fruit and vegetables, drinking cups, and for overwrap and lamination films. As the use of PLA expands to a broader range of products, research that accounts for the variation of barrier properties of PLA as a function of water activity is necessary. The aim of this work was to study the variation in the oxygen diffusion, solubility, and permeability coefficient of polyethylene terephthalate, PET, and PLA films at different temperatures (5, 23, and 40°C) and water activities (0 to 0.9). The water sorption isotherm for PLA films was also determined. Diffusion coefficients were determined using the "half-sorption time" method and a consistency test for continuous flow permeability experimental data. The permeability coefficients were obtained from steady state permeability experiments. Results indicated that PLA films absorb very low amounts of water and no significant variation of the absorbed water with temperature was found. Oxygen permeability coefficients obtained for PLA films (2 to 12 x 10^{-18} Kg.m/m^2.s.Pa) were higher than those obtained for PET films (1 to 6 x 10^{-19} kg.m/m^2.s.Pa) at different temperatures and water activities. Moreover, permeability coefficients for PLA and PET films did not change significantly with changes in water activity at temperatures lower than 23°C.
Keyword: Poly(lactide); permeability; oxygen diffusion; solubility; water sorption.

Introduction

Poly(lactide), PLA, polymers derived from lactic acid (2-hydroxypropionic acid) are ready to be adopted as polymeric packaging materials. PLA has been widely studied for use in medical applications because of its bioresorbable and biocompatible properties in the human body [1-7]. Due to its higher cost, the initial focus of PLA as a packaging material has been in high value films, rigid thermoforms, food and beverage containers, and coated papers. As modern and emerging technologies of producing PLA are lowering production costs [8,9], PLA may have packaging applications for a broad array of products; moreover, new applications such as fibers are being pursued [10].

Early economic studies show that PLA is an economically feasible material to use as packaging polymer [8]. Medical studies reported that the level of lactic acid, LA, that migrates to food from packaging containers is much lower than the amount of LA used in common food ingredients [11]. Therefore, polymers derived from lactic acid are good candidates for packaging applications [2,5,12]. Currently, PLA is being used as a food packaging polymer for short shelf life products with common applications such as containers, drinking cups, sundae and salad cups, overwrap and lamination films, and blister packages [13,14]. In the next five years, PLA production and consumption is expected to increase [8,13,15-19]. So, research into the variation of physical, mechanical, and barrier properties in PLA polymers is necessary.

One of the main concerns for packaging polymers is to assess how they perform under real and differing environmental conditions (i.e., refrigerated, standard, and tropical). Water-polymer interactions play a significant role in the general properties and aging of polymers. It is well known that the presence of water has a significant effect on barrier and mechanical properties of most hydrophilic polymers. The presence of water or other small molecular mass compounds in the polymer matrix may change the way that a gas or vapor is sorbed and diffused through the polymer [20]. For example, in the case of oxygen diffusion in hydrophilic polymers, the presence

of water molecules that interact with the polymer matrix influences the mass flow rate of the oxygen [20,21]. In the case of hydrophobic polymers or polymers free of hydrogen bonding groups, such as poly(ethylene terephthalate) (PET) and PET-like polymers (e.g., PLA since it has helix structures and bulky side-chains [2]). The water equilibrium concentration in saturated conditions is typically lower than 2% by weight.

The room temperature isotherm for PET films was reported as a typical sigmoidal shape with a water absorption lower than 1.0% at water activity (A_w) higher than 0.9 [22]. For PLA pellets, Witzke reported an absorption less than 8000 ppm (wt/wt) at A_w= 0.9 [23]. So, in polymers such as PET and PLA that absorb very low amounts of water, the effect of water can also be crucial to the polymers' barrier properties and general performance. For example, in the case of PET, water plasticizes the amorphous phase, which leads to a decrease of the T_g from about 80°C in a dry state to about 57°C in a saturated state and with a consequent reduction of the elastic modulus [24]. Also, for PLA a significant change of the glass transition temperature as a function of water content was reported [25]. Besides the changes in physical and mechanical properties, surprising changes in polymer barrier properties and diffusion mechanism can happen as a result of the presence of relatively small quantities of absorbed water. In PET, early studies show that the diffusion coefficient follows Fick's first law [26], and that the oxygen solubility follows Henry's law [27]. Since the presence of water has a significant effect on the mechanical and barrier properties, PET and PLA polymers may show a variation of the oxygen permeability coefficient as water content increases. The aim of this work was to study the variation of the oxygen diffusion, solubility, and permeability coefficient of PET and PLA films at different temperatures (5, 23, and 40°C) and water activities (0 to 0.9). The water sorption isotherm for PLA films was determined. The glass transition temperature, melting temperature and crystallinity of PLA and PET polymers was also measured.

Materials

Poly(lactide) film identified as 4031-D was provided by Cargill-Dow LLC Polymers. 4031-D was made with nominally 98% of L-Lactide; density was around 1,250 kg/m^3. Standard PET film was used to measure the PET barrier properties. Films were studied as received.

Methods

Thickness. Thickness of films was determined with a TMI 549M micrometer (Testing Machines, Inc., Amityville, NY) according to ASTM D374 – 99.

Thermal Characterization. A differential scanning calorimeter (DSC 2010) from TA Instruments (New Castle, DE) was used to determine T_g and T_m (ASTM D 3418 – 97); and enthalpies of fusion (ΔH_f) and crystallinity of PLA and PET polymers (ASTM D 3417 – 97).

Water Sorption Isotherm. Saturated salt solutions of lithium chloride, magnesium chloride, magnesium nitrate, sodium chloride, potassium chloride, and potassium nitrate were used to provide A_w of 0.11, 0.33, 0.52, 0.75, 0.85, and 0.94 respectively. All chemicals were analytical grade obtained from EM-Science. The above-saturated solutions were put into different desiccators in which the samples were added. Sorption experiments were carried out with film specimens of size 0.5 cm x 3 cm. The initial moisture content (IMC) of the PLA films (in triplicate) was measured on a dry-weight basis by drying in a hot-air vacuum oven at 60°C for 10 hr. The samples were weighed until equilibrium (± 0.0001 g) and a Metrohm Karl Fischer Titrator K 720 from Metrohm Ltd. Herisau (Switzerland) was used to determine the final moisture content.

Oxygen Permeability. A modified Oxtran 100 – Twin with a coulometric sensor, from Mocon Inc., Minneapolis, MN, was used for measuring permeability of oxygen through the polymer films as a function of water activity. The experiments were carried out at 0.21 atm pressure for PLA films and 1 atm pressure for PET films. Figure 1 shows a schematic diagram of the test apparatus, similar to one used by previous researchers [21]. Before mounting the polymer film in the cell, the film was vacuum dried at 60°C for at least 10 hours. After the films were mounted to cell A and B (Figure 1), a stream of dry nitrogen was circulated through the system. For each water activity value at which the permeability of oxygen was measured, a nitrogen stream adjusted to the selected water activity flowed throughout the cell containing the film for at least 24 h.

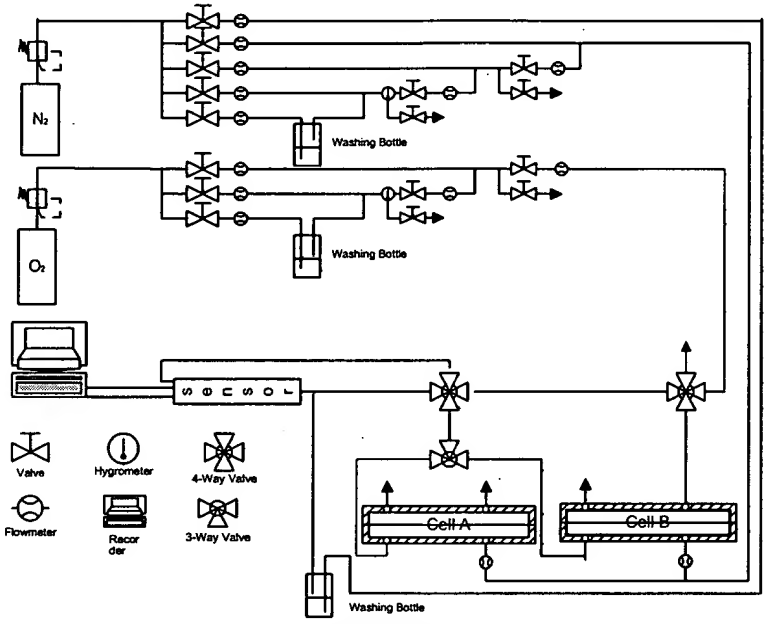

Figure 1. Schematic diagram of the test apparatus for permeability experiments

During this period, the film acquired moisture content in equilibrium with that in the nitrogen stream. Initial time was marked when an oxygen gas stream at the selected water activity, equal to the water activity of the film in the cell, was introduced. The amount of oxygen permeated per unit of time was continuously monitored with a Mocon integrator Model D-200, Mocon Inc., Minneapolis, MN, until a steady state was reached (i.e., the oxygen flux changed by less than 1% for 30 minutes). The instrument was calibrated at each temperature that the samples were tested (i.e., 5, 23, and 40°C) by measuring the oxygen flow rate through a standard reference material provided by Mocon Inc., Minneapolis, MN. Water activity values were determined by using a Hygrodynamics' Wide Range Humidity Sensor model 1820A from Newport Scientific, Inc, MD. The experimental error in the determination of oxygen flow rate on the Oxtran 100 – twin apparatus was estimated at 2 to 5%, with highly reproducible and consistent readings. The experimental error in the measurement of the water activity was estimated at 2%.

Theoretical Background; The data obtained were analyzed by a consistency test for isostatic permeability experiments [28]. This test permits the detection of any significant variation of temperature and concentration during the experiment, and it also provides information about the diffusion and sorption mechanism of the oxygen in the polymer. At the beginning of the permeation process (i.e., transient state) the oxygen concentration is changing with time. After

that, the permeation process reaches a steady state where the oxygen concentration is independent of time. The solution of the amount of oxygen that permeates a thin sheet can be obtained from the general diffusion Equation (1)

$$F = -D \nabla c \tag{1}$$

When the diffusion coefficient (D) is independent of concentration (C) (usually true in polymers above their Tg) the one dimensional solution of equation (1) can be expressed as equation 2 which describes the process mentioned above with boundary conditions according to Fick's second law [29] for a film sheet tested by an isostatic permeation experiment [28].

$$\frac{F_t}{F_\infty} = \left(\frac{4}{\sqrt{\pi}}\right)\left(\sqrt{\frac{l^2}{4Dt}}\right)\sum_{n=1,3,5,..}^{\infty} \exp\left(\frac{-n^2 l^2}{4Dt}\right) \tag{2}$$

where F_t is the flow rate of oxygen permeating the film at the transient state at time t, F_∞ is the oxygen transmission rate at the steady state, l is the film thickness, and D is the oxygen diffusion coefficient. To apply the consistency test, Equation (2) is simplified to Equation (3), which describes the permeation for a flow ratio from 0.05 to 0.95 [28].

$$\phi = \frac{F_t}{F_\infty} = \left(\frac{4}{\sqrt{\pi}}\right) X^{1/2} \exp(-X) \tag{3}$$

where $X=l^2/4Dt$, and ϕ is the ratio between the flow rates at time t and at steady state. From the isostatic method, ϕ is obtained from time zero until the polymer reaches steady state. So, by using a Newton-Raphson method [30] the value of X can be calculated for each value of t and the diffusion coefficient D can be obtained from the slope of 1/X versus time . The plot of 1/X as a function of time is expected to be a straight line, which intercepts the origin of both axes. By this method, it is also possible to determine two constants (i.e., K_1 and K_2), which are the ratio of the X values at $\phi = 0.50$ and 0.75 divided by the value of X at $\phi = 0.25$. If an error level of 5% is considered acceptable, the values obtained for these two constants are as follow: $0.42 \leq K_1 \leq 0.46$ and $0.65 \leq K_2 \leq 0.69$ [28,31]. Calculation of K_1 & K_2 permits evaluation of whether the isostatic tests were carried out at the right conditions and also checks the diffusion mechanics that take place. In addition, from the flow transient rate profile, the half-time diffusion coefficient, D, can be estimated from Equation (4) [29].

$$D = \frac{l^2}{7.199 * t_{0.5}} \tag{4}$$

After that, a procedure based on the sum of squares technique was applied to determine the best estimated diffusion coefficient value from Equation (2) [32]. Next, the diffusion coefficients obtained for the continuous flow method and from the sum of squares were compared. The steady state time was calculated by solving Equation (2) when ϕ is equal to one with the diffusion coefficient obtained from the previous step. Using the value of permeant flow at steady state F_∞, the permeability coefficient P was determined by Equation (5).

$$P = \frac{F_\infty l}{A \Delta p} \tag{5}$$

where A is the area of the film, and Δp is the partial pressure gradient across the polymer film. Then, if Henry's law of solubility is applied in the case of oxygen diffusion in films at low pressure (i.e., up to one atmosphere) the solubility coefficient S, can be calculated from,

$$P = S \cdot D \tag{6}$$

The temperature dependence of P, S, and D can be described by a Van't Hoff's - Arrhenius equation [33].

$$S(T) = S_0 \exp(-\Delta H_S/RT) \quad (7)$$
$$D(T) = D_0 \exp(E_D/RT) \quad (8)$$
$$P(T) = P_0 \exp(-E_P/RT) \quad (9)$$

Where ΔHs is the molar heat of sorption, E_D is the activation energy of diffusion, and E_p is the apparent activation energy of permeation.

Results & Discussion

Thickness. Since the main source of error in calculating the diffusion coefficient, Equation (4) and the permeability coefficient, Equation (5), is the thickness, special care was taken to determine the film thickness. The thickness of PLA and PET films was determined according to ASTM D 374 – 99. For 4031, it was 23.2 μm (0.913 mil), and for PET, thickness was 23.4 μm (0.921 mil).

Thermal Characterization. Poly(lactide) films undergo an endothermic event which is superimposed on T_g and observed during the first DSC heating [12]. This endothermic relaxation is indicated in Table 1. Also Table 1 presents the glass transition and melting temperatures and the enthalpy of fusion for both PLA and PET films. The percent crystallinity, x_c, can be evaluated as follows: $x_c = 100 \cdot \Delta H_m / \Delta H_m^c$. where ΔH_m is the enthalpy of fusion and ΔH_m^c is the heat of melting of purely crystalline poly(L-lactide) or PET. For PLA, ΔH_m^c =93 J/g [34], and for PET, ΔH_m^c =125.6 J/g [35]. PLA 4031-D shows lower T_g and T_m than PET films.

Table 1. DSC results for PLA and PET

	4031-D	**PET**
T_g, °C	71.4	80
Relaxation enthalpy, J/g	1.4	N/A
Tm, °C	163.4	245
Enthalpy Fusion, J/g	37.5	47.7
Percent Crystallinity	40	38

Water Sorption Isotherm. PLA films stored for more than one week at 5, 23, and 40°C and a_w of 0.11, 0.33, 0.52, 0.75, 0.85, and 0.94 respectively were periodically weighed with a precision of ± 0.0001 g and dried in a vacuum oven. Since the average samples were around 0.2 g, a water absorption value of 500 ppm could be detected by this technique. The Metrohm Karl Fischer Titrators K 720 equipment can measure water absorption with a sensitivity of 100 ppm. Neither technique was able to measure water absorbed in PLA under any A_w.

Having 33% acyl ester bonds in its backbone, PLA is more susceptible to hydrolysis than many commercial types of polyester. Previous studies in amorphous poly(lactide) pellets (M_n = 50,000-100,000 Daltons) with a porosity of 8.24%, total pore area of 36.8 m^2/g, and an average pore diameter of 0.0072 μm indicated low amounts of water absorption (i.e., 8000 ppm at 25°C and A_w=0.9, with an equilibrium time no higher than 72 hr) [23]. Also, the same researchers reported that water absorption is fairly insensitive to moderate temperature changes. PLA is moderately polar with a solubility parameter (δ) of 19 - 20.5 $MPa^{0.5}$ [4]. The solubility parameter of water is 48 $MPa^{0.5}$. When the difference between the solubility parameters of the water and the polymer is higher, the water sorption decreases. For PET the δ is 16 $MPa^{0.5}$ and the water absorption is 60 ppm at 25°C at A_w=0.5. For PS (δ=19 $MPa^{0.5}$) the water absorption is 320 ppm at 25°C at A_w=0.5 [23]. So, in the case of PLA an amount of water absorbed between the value

absorbed for PET and PS films is expected. However, we were not able to measure water absorption in either of the PLA films studied. Some of the difference between the amounts of water absorbed by the pellets and the films could be explained by the differences in crystallinity; in addition, some of the water measured in the pellets could be trapped in the porous structure, rather than absorbed in the PLA. Since low water content at equilibrium is expected for PLA films, further research with more sensitive instrumentation is needed.

Oxygen permeability. The diffusion, solubility, and permeability coefficients of PET and PLA were determined by the isostatic technique at 1 and 0.21 atmospheres pressure, three temperatures (5, 23, and 40°C), and water activities of 0, 0.3, 0.6 and 0.9. Four different water activities were selected since PET and PLA films do not absorb much water and also do not show much variation of water absorbed as temperature increases [12,25].

Polyethylene terephthalate

Representative plots of oxygen permeation as a function of time are presented in Figure 2 a) for PET films at 5°C, 23°C, and 40°C at A_w=0.9, and in Figure 2 b) for PET films at 40°C and A_w= 0, 0.3, 0.6, and 0.9.

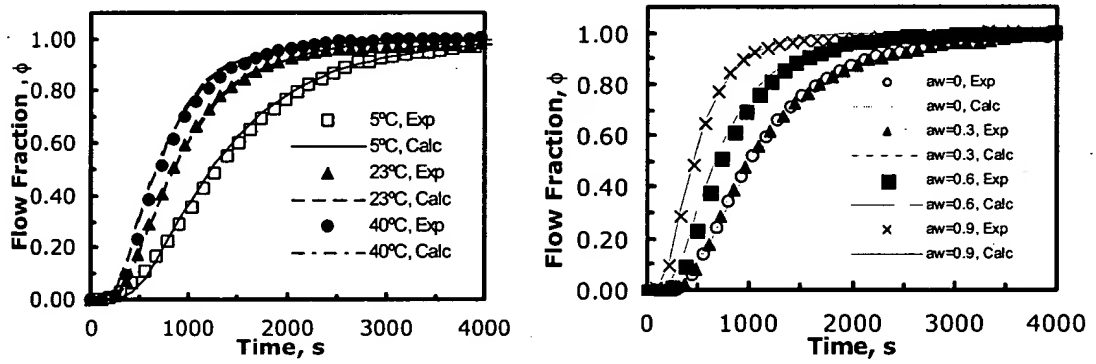

Figure 2 a & b. a) Permeant flow fraction versus time for oxygen permeation experiment for PET films at 5, and 40°C, A_w=0.6. **b)** Permeant flow fraction versus time for oxygen permeation experiment for PET films at 40°C, and A_w=0, 0.3, 0.6, and 0.9.

Figure 2 a & b show a faster transient state as water activity and temperature increased. Figure 2 b also shows that not much variation of the oxygen flow fraction was found at water activity lower than 0.3. The behaviors shown in Figure 2 a & b were found at the three different temperatures at which the polymers film were tested. In both figures, a good correlation between the experimental and calculated values by equation (2) can be observed.

The permeability coefficients at different water activities and temperature were calculated by using equation (5) (see Figure 4 a). Figure 4 a shows that the values of oxygen permeability coefficients decrease as temperature decreases. The oxygen permeability coefficient tended to decrease as the water activity in the oxygen stream increased, which is the opposite effect shown by hydrophilic polymers [20]. This decrease of the oxygen permeability coefficients was more significant at 40°C than at 23°C and 5°C. The values of permeability coefficients obtained in this research are similar to the values found in the literature [36]; however, they are a little lower. (e.g., oxygen permeability coefficient of PET reported in the literature 7.64×10^{-19} kg.m/m2.s.Pa at 25°C at A_w=0 [36]). This can be explained by the difference in crystallinity and final polymer treatment Values of the oxygen diffusion coefficient versus water activity obtained from the unsteady state by the consistency test for isostatic permeability experiments are shown in Figure

4 b. An exponential increase in the diffusion coefficient as water activity increases is observed, and an increase in the oxygen diffusion coefficient as the water activity increases is also evidenced. This effect is also more pronounced at 40°C than at 23°C and 5°C.

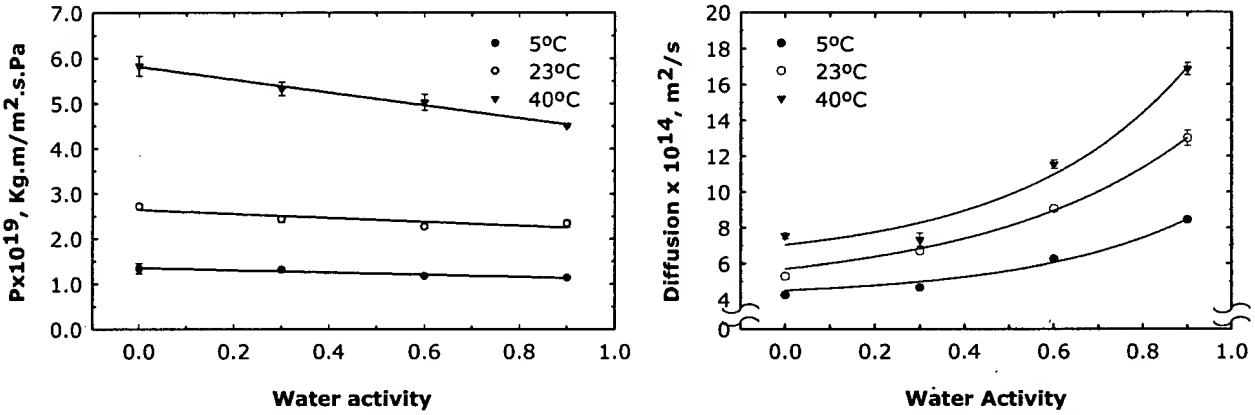

Figure 4 a & b. a) PET oxygen permeability coefficient versus water activity at 5, 23, and 40°C. **b)** Diffusion coefficient of PET films as a function of water activity

The increase of oxygen diffusion coefficient at higher water activity content can be attributed to a major plasticization effect of the amorphous PET phase by the water molecules. The plasticization effect, as in hydrophilic polymers, tends to increase the mobility of the oxygen molecules in the polymer bulk phase. This plasticization effect is evidenced by the reduction of the T_g. For PET, water plasticization leads to a decrease of the T_g from about 80°C in the dry state to about 57°C in the saturated state [24]. Although PET shows a reduction of the glass transition temperature, clustering of water molecules was not reported [37]. Thus, if we compare the values of diffusion coefficient obtained in this research at 25°C and 40°C, they are one order of magnitude lower than the values found in the literature [36]. This can be explained by different crystallinity and processing conditions of the films used (i.e., Oxygen diffusion coefficient of PET reported in the literature5.6×10^{-13} m^2/s at 25°C at A_w=0, and 11.6×10^{-13} m^2/s at 40°C at A_w=0 [36]).

Figure 5 presents the values of solubility coefficient versus water activity for PET films at 5°C, 23°C, and 40°C. An increase of the solubility coefficient as temperature increased was observed, and a reduction of the solubility coefficient as water activity increase was evident. Henry's law is obeyed for PET films in the range of 0 to 1.0 atm [27]. However, the contribution of the Henry's law mechanism is small in PET films. Rather, sorption is the process of filling the holes of free volume, and the solubility should be proportional to the amount of free volume [36,38,39]. Since PET solubility is directly proportional to the free volume of the amorphous polymer matrix [26], a reduction of the free volume available will produce a decrease in the solubility. So, the linear variation of the solubility coefficient as water activity increased can be explained by a competition between the water and oxygen molecules for the free volume. When water activity increased and as a consequence so did the amount of water sorbed in the polymer, the solubility of oxygen decreased. Since the permeation of water in PET polymers is faster than the oxygen permeation (i.e., water permeability is $P=1.1 \pm 0.1\times10^{-15}$ Kg.m/m2.s.Pa at 25°C between A_w 0.4 and 0.9 [12]), the free volume is first filled with water molecules and then with oxygen.

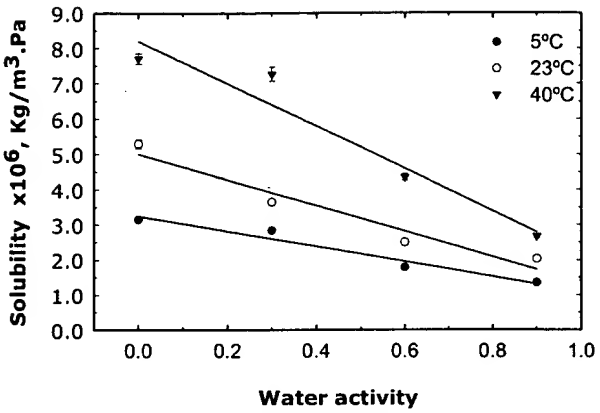

Figure 5. Solubility coefficient of PET films as a function of water activity.

Therefore, the net effect of the presence of water would be an increase of the diffusion coefficient and a reduction of the solubility coefficient. Similar behavior was observed in PET films in mutual permeation of nitrogen and oxygen [40]. Since the oxygen diffused faster than the nitrogen, the solubility of nitrogen decreased and the diffusion of nitrogen increased as oxygen concentration increased. The values of solubility coefficient obtained in this research are higher that the values found in the literature (i.e., Oxygen solubility coefficient of PET reported in the literature $1.38x10^{-6}$ $Kg/m^3.Pa$ at 25°C at $A_w=0$ [36]); however, this could be due to the difference in crystallinity and processing conditions.

Poly(lactide) 4031

Figure 6 a represents the oxygen permeability coefficient for PLA polymers as a function of the water activity. A significant increase of the oxygen permeability coefficient as temperature increased can be observed for PLA 4031. PLA 4031 shows an increase of the oxygen permeability coefficient from 3.5×10^{-18} $Kg.m/m^2.s.Pa$ at 5°C to 11×10^{-18} $Kg.m/m^2.s.Pa$ at 40°C when moisture is not present. Under higher water activity levels ($A_w=0.9$), the value of the oxygen permeability coefficient increases only to 8.5×10^{-18} $Kg.m/m^2.s.Pa$ at 40°C. This reduction of the oxygen permeability coefficient as water activity increased at a constant temperature is observed in Figure 6 a for the three temperatures tested. The reduction of values is more pronounced at 40°C. The difference between the values of oxygen permeability measured in this research, and the values measure in previous studies [6] of $3.53x10^{-17}$ $Kg.m/m^2.s.Pa$ at 30°C and $A_w=0$ for PLA biaxially oriented films can be explained by the differences in the crystallinity and final processing conditions of both films. The oxygen diffusion coefficient of 4031 is presented in Figure 6 b. A similar behavior to the one shown for PET films in Figure 4 b is observed for PLA films. As for PET films, the oxygen diffusion coefficient increased as the temperature increased. Also an exponential increase of the oxygen diffusion coefficients from $2x10^{-14}$ to $9x10^{-14}$ m^2/s at 23°C can be observed as water activity increased from 0 to 0.9. The observed increase of the oxygen diffusion coefficient in the range of $A_w=0$ to 0.9 can also be attributed to the plasticization effect on the amorphous phase by the water molecules. As in PET, plasticization effects tend to increase the mobility of the oxygen molecules in the polymer matrix. Plasticization effects are evidenced by a reduction of the polymers T_g. In previous work

[25], it was shown that the variation of the glass transition temperature was significant when the samples were stored for seven days at 5, 23, and 40°C and different relative humidities.

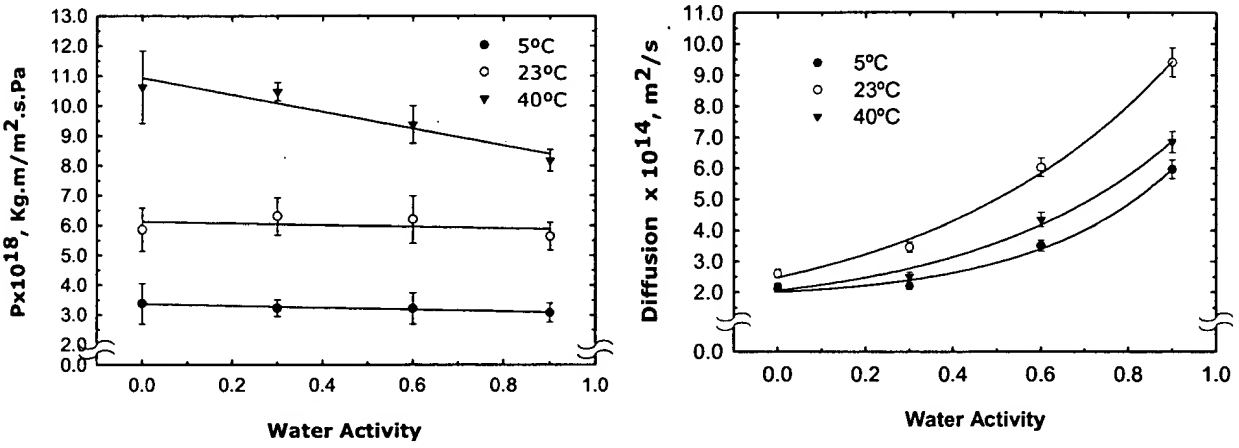

Figure 6 a & b. a) Oxygen permeability coefficient as a function of water activity for PLA 4031. b) Oxygen Diffusion Coefficient of 4031 films as a function of water activity

Some authors attribute this reduction of glass transition temperature in hydrophilic films to clustering of water in the polymer matrix [20]. However, in the case of PLA and other hydrophobic films, clusters of water were not reported in the polymer matrix [23,36,38].

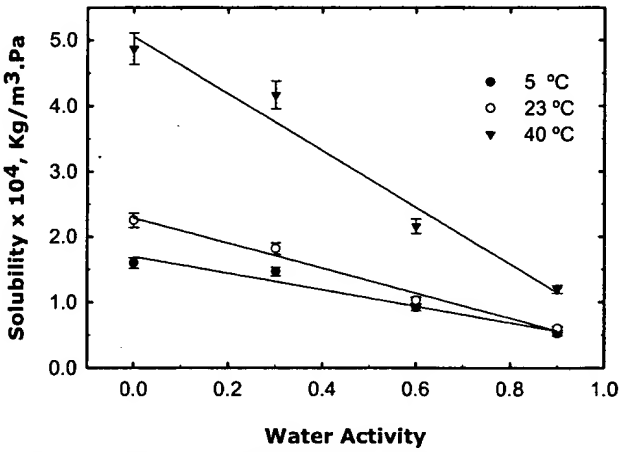

Figure 7. Solubility Coefficient of PLA 4031 films as a function of water activity.

Figure 7 presents the values of oxygen solubility coefficient in PLA 4031. The oxygen solubility coefficient increases as the temperature increases. A linear reduction of the solubility coefficient from 5 to $1.5x10^{-4}$ $Kg/m^3.Pa$ at 40°C can be observed as water activity increased from 0 to 0.9. This reduction can be explained, as in the case of PET, by the occupancy of the free volume by water molecules at higher water content, so a reduction of the oxygen solubility as water content increased is observed.

The enthalpies of sorption, ΔHS, the activation energy of diffusion, E_D, and the apparent activation energy of permeation, E_P, were calculated using Equation (7, 8, and 9). The results are presented in Table 2.

Table 2. Pre-exponential terms of equation (7, 8, and 9) and enthalpy of sorption, activation energy for diffusion and permeation in the oxygen mass transport through PET and PLA films at different water activity conditions.

Material	Water Activity	P_0x10^{14}, Kg.m/m^2.s.Pa	E_P, KJ/mol	D_0x10^{12}, m^2/s	E_D, KJ/mol	S_0x10^3 Kg/m^3.Pa	ΔH_S, KJ/mol
PET	0.0	6.24	30.30	6.63	11.76	9.68	18.54
	0.3	2.99	28.60	2.9	9.47	10.2	19.13
	0.6	4.75	29.93	10.1	11.62	4.69	18.31
	0.9	2.41	28.36	38.9	14.22	0.62	14.14
4031	0.0	9.00	23.62	300.00	0.96	2667.80	22.65
	0.3	12.4	24.38	981.00	3.18	1264.44	21.19
	0.6	4.86	22.18	34.20	4.97	141.901	17.21
	0.9	2.00	20.24	27.84	3.29	72.04	16.94

The average apparent activation energy of permeation for PET are on the order of E_P =29.3 ± 0.96 KJ/mol, and P_o= 4.09 ± 1.74 Kg.m/m^2.s.Pa. The activation energy of diffusion increases from 11.76 KJ/mol at A_w=0 to 14.22 KJ/mol at A_w=0.9. An increase in the values of the oxygen diffusion activation energy indicates that the diffusing molecule must overcome larger intermolecular forces within the polymer at higher water contents to diffuse. Together with the increase of activation energy of diffusion, a reduction of the enthalpy of sorption can be observed at higher humidity contents. If we compare the values of the activation energy of permeation with the values reported in the literature [41], Ep=32 KJ/mol at A_w=0, a good agreement can be seen. The apparent activation energy of permeation for PLA 4031 is mainly constant between A_w=0 and 0.6, E_P =23.39 ± 1.11 KJ/mol. However, a reduction of the activation energy at A_w=0.9 of almost 2 KJ/mol is evidenced. The activation energy of diffusion increases from 0.96 KJ/mol at A_w=0 to 3.29 KJ/mol at A_w=0.9, with the major increase between A_w=0 and 0.3. If we compare the values of activation energy between 4031 and PET we can see that PLA presents less resistance to oxygen diffusion than PET. Also the increase of the activation energy of diffusion is accompanied by a reduction in the enthalpy of sorption for PLA 4031 from 22.65 KJ/mol at A_w=0 to 16.94 KJ/mol at A_w=0.9. The difference between the oxygen permeation activation energy measured in this research and the one reported in previous research [6] (Ep= 11.2 KJ/mol at A_w=0) may be explained by the difference in the polymer crystallinity and processing conditions). Finally, PET and PLA both are hydrophobic films that absorb very low amounts of water, and show the same kind barrier property behavior, as was shown in this research.

Conclusions

The oxygen barrier properties of PET and PLA films at three different temperatures, 5°C, 23°C, and 40°C, were measured. The permeability coefficients of PET and PLA decreased as the water content was increased. An increase of the permeability coefficient of PET and PLA was observed as temperature increased. Oxygen diffusion of PET and PLA showed an exponential increase as water activity increased at each temperature. The effect is more pronounced at higher temperature. The oxygen solubility coefficient decreased linearly as the water activity increased, due to the reduction in free volume because of its occupation by the water molecules.

Acknowledgments

We thank Kraft Foods for partially supporting this project and Cargill Dow LLC for the polymer samples

Reference

(1) Mainil-Varlet, P.; Curtis, R.; Gogolewski, S. *Journal of Biomedical Materials Research* **1997**, *36*, 360-380.
(2) Ikada, Y.; Tsuji, H. *Macromolecular Rapid Communications* **2000**, *21*, 117-132.
(3) Bleach, N. C.; Tanner, K. E.; Kellomaki, M.; Tormala, P. *Journal of Materials Science: Materials in Medicine* **2001**, *12*, 911-915.
(4) Tsuji, H.; Sumida, K. *Journal of Applied Polymer Science* **2001**, *79*, 1582-1589.
(5) Dorgan, J. R.; Lehermeier, H. J.; Palade, L.-I.; Cicero, J. *Macromolecular Symposia* **2001**, *175*, 55-66.
(6) Lehermeier, H. J.; Dorgan, J. R.; Way, D., J. *Journal of Membrane Science* **2001**, *190*, 243-251.
(7) Benicewicz, B. C.; Hopper, P. K. *Journal of Bioactive and Compatible Polymers* **1995**, *5*, 453-472.
(8) Dattaa, R.; Tsaia, S.-P.; Bonsignorea, P.; Moona, S.-H.; Frank, J. R. *FEMS Microbiology Reviews* **1995**, *16*, 221-231.
(9) Drumright, R. E.; Gruber, P. R.; Henton, D. E. *Advanced Materials* **2000**, *12*, 1841-1846.
(10) Perepelkin, K. E. *Fibre Chemistry* **2002**, *34*, 85-100.
(11) Conn, R. E.; Kolstad, J. J.; Borzelleca, J. F.; Dixler, D. S.; Filer Jr, L. J.; LaDu, B. N.; Pariza, M. W. *Fd Chem. Toxic* **1995**, *33*, 273-283.
(12) Auras, R.; Harte, B.; Selke, S.; Hernandez, R. Worlpack 2002, East Lansing, MI, USA, **2002**; p 1011-1021.
(13) Whiteman, N. Packexpo, Chicago, IL, **2002**; p 37-42.
(14) Baillie, J. In *Packaging Week*, **1997**; Vol. 13.
(15) Mohan, A. M. In *Packaging Digest*, **2002**. 30 -32
(16) Nageroni, J. *Flexible Packaging* **2001**, 25-26.
(17) Michael, O. B.;; Cargill Dow LLC:, **2002**; Available at http://www.cargilldow.com/corporate/news_archives.asp.
(18) O'Brien, M.;; Cargill Dow LLC:, **2003**; Available at http://www.cargilldow.com/corporate/news_archives.asp
(19) O'Brien, M.;; Cargill Dow LLC:, **2003**; Available at http://www.cargilldow.com/corporate/news_archives.asp
(20) Hernandez, R. J. *Journal of Food Engineering* **1994**, *22*, 495-507.
(21) Gavara, R.; Hernandez, R. J. *Journal of Polymer Science* **1994**, *32*, 2375-2382.
(22) Ravens, D. A. S.; Ward, I. M. *Trans. Faraday Society* **1960**, *57*, 150.
(23) Witzke, D. R. Doctor of Philosophy, Michigan State University, **1997**.
(24) Launay, A.; Thominette, F.; Verdu, J. *Journal of Applied Polymer Science* **1999**, *73*, 1131-1137.
(25) Auras, R.; Harte, B.; Selke, S. ANTEC 2003, Nashville, TN, **2003**. To be presented.
(26) Michaels, A. S.; Vieth, W. R.; Barrie, J. A. *Journal of Applied Physics* **1963**, *34*, 13-20.
(27) Michaels, A. S.; Vieth, W. R.; Barrie, J. A. *Journal of Applied Physics* **1963**, *34*, 1-12.
(28) Gavara, R.; Hernandez, R. J. *Journal of Plastic Film & Sheeting* **1993**, *9*, 126-138.
(29) Crank, J. *The Mathematics of Diffusion*; Oxford University Press: Grean Britain, **1975**.
(30) Chapra, S. C.; Canale, R. P. *Numerical Methods for Engineers; with programming and software applications*; Third Edition ed.; McGraw-Hill, Inc, **1998**.
(31) Hernandez-Munoz, P.; Gavara, R.; Hernandez, R. J. *Journal of Membrane Science* **1998**, 1-10.
(32) Barr, C. D.; Giacin, J. R.; Hernandez, R. J. *Packag. Technol. Sci.* **2000**, *13*, 157-167.
(33) VanKrevelen D.W. *Properties of Polymers*; Third ed.; Elsevier Science B.V.: Amsterdan, The Netherlands, 1997.
(34) Fischer, E. W.; Sterzel, H. J.; Wegner, G. *Kolloid-Z. u. Z. Polymere* **1973**, *251*, 980-990.
(35) Wunderlich, B. *Macromolecular Physics*; Academic Press: New York, **1973**.
(36) Polyakova, A.; Liu, R. Y. F.; Schiraldi, D. A.; Hiltner, A.; Baer, E. *Journal of Polymer Science: Part B: Polymer Physics* **2001**, *39*, 1889-1899.
(37) Shigetomi, T.; Tsuzumi, H.; Toi, K.; Ito, T. *Journal of Applied Polymer Science* **2000**, *76*, 67-74.
(38) Polyakova, A.; Connor, D. M.; Collard, D. M.; Schiraldi, D. A.; Hiltner, A.; Baer, E. *Journal of Polymer Science Part B: Polymer Physics* **2001**, *39*, 1900-1910.
(39) Sekelik, D. J.; Stepanov, E. V.; Nazarenko, S.; Schiraldi, D.; Hiltner, A.; Baer, E. *Journal of Polymer Science Part B: Polymer Physics* **1999**, *37*, 847-857.
(40) Lewis, E. L. V.; Duckett, R. A.; Ward, I. M.; Fairclough, J. P. A.; Ryan, A. J. *Polymer* **2003**, *44*, 1631-1640.
(41) Hernandez, R. J.; Selke, S. E. M.; Culter, J. D. *Plastics Packaging*; Hanser: Munich, **2000**.